

The Effect of Rabi Frequency on the Electric Susceptibility of the Six-levels Inverted-Y Atomic Systems

<http://www.doi.org/10.62341/ssei2035>

Suad A. Almjar, Eman O. Mafaa, Suad M. Abuzariba, Issra M. Bunhmada
Physics Department, Faculty of Science, Misurata University-Libya
Suadabu@yahoo.com

Abstract

The effect of changing the value of Rabi frequency has been studied in six level atomic system, Optical Bloch equations were used as the main tool to get the final shape of the model to treat the model. In this work we present a theoretical study of the non-linear optical properties of materials as a result of their interaction with laser radiation in resonance state. Density matrix was used in our formulation of Optical Bloch Equation. These equations were solved using Matlab program for Six-levels Inverted-Y Atomic Systems. A formula for calculation of electrical susceptibility was obtained. With increasing the real and imaginary parts of the electric susceptibility have also increased gradually which effects the index of refraction of the medium (real part), and the absorption window (described by the imaginary part). Moreover, when increasing the real and imaginary parts of the electric susceptibility decreased and we noticed that with increasing the value of the signal laser field related to transition $|2\rangle \leftrightarrow |6\rangle$ a distortion starts to appear on both real and imaginary parts.

Key Words: Rabi frequency, Density matrix, electrical susceptibility, laser, Optical Bloch equations.

تأثير تردد رابي على القابلية الكهربائية لأنظمة الذرية من نوع Υ المقلوبة ذات الستة المستويات

سعاد ابوالقاسم مجاور، ايمان عمر معافى، سعاد محمد ابوزربية، اسراء محمد بن احميدة

قسم الفيزياء - كلية العلوم - جامعة مصراتة

Suadabu@yahoo.com

الملخص

تم دراسة تأثير تغيير قيمة تردد رابي في نظام ذري بستة مستويات، حيث تم استخدام معادلات بلوخ الضوئية كأداة رئيسية للحصول على الشكل النهائي للنموذج لمعالجة النموذج. في هذا العمل نقدم دراسة نظرية للخصائص البصرية غير الخطية للمواد نتيجة تفاعلها مع إشعاع الليزر في حالة الرنين. تم استخدام مصفوفة الكثافة في صياغتنا لمعادلة بلوخ الضوئية. تم حل هذه المعادلات باستخدام برنامج ماتلاب لأنظمة الذرية ذات الستة مستويات المقلوبة Υ . تم الحصول على صيغة لحساب القابلية الكهربائية. مع زيادة الأجزاء الحقيقية والتخيلية للقابلية الكهربائية زادت أيضاً تدريجياً مما يؤثر على معامل انكسار الوسط (الجزء الحقيقي) ونافاذة الامتصاص (الموصوفة بالجزء التخيلي). علاوة على ذلك، عند زيادة الأجزاء الحقيقية والتخيلية انخفضت القابلية الكهربائية ولاحظنا أنه مع زيادة قيمة مجال إشارة الليزر المتعلقة بالانتقال $|2\rangle \leftrightarrow |6\rangle$ يبدأ التشويه في الظهور على كل من الأجزاء الحقيقية والتخيلية. **الكلمات المفتاحية:** تردد رابي، مصفوفة الكثافة، القابلية الكهربائية، الليزر، معادلات بلوخ الضوئية.

Introduction:

Nonlinear optics is one of the important issues in optics. Nonlinear optical properties refer to the changes in a material's response when it interacts with high-intensity light. This interaction modifies the material's optical properties, transitioning from a linear to a nonlinear response. The interaction of light with matter has been studied in both quantum [1, 2], and semiclassical treatments [3]. In the semiclassical approach, atoms are treated quantum mechanically, where all the fields are treated as classical vector fields [4]. Nonlinear electric susceptibility one of the nonlinear properties, it contains both real and imaginary parts, the real part related to the index of refraction, and the imaginary part related to the absorption. The nonlinear absorption and refraction in multilevel system described by density matrix [5, 6]. In its simplest configuration, two electromagnetic fields excite an ensemble of three-level atoms in Λ configuration and the optical properties of the atomic medium are described by the first-order complex electric susceptibility χ^1_{ϵ} . Its real part $\text{Re}\{\chi^1_{\epsilon}\}$ is related to the index of refraction of the medium, the absorption

window is described by the imaginary part $\text{Im}\{\chi^1_{\epsilon}\}$ [7, 8]. Furthermore, there are several studies on the four and five levels systems and their applications [9-13]. The effect of the Rabi frequency on the electric susceptibility for Λ -type atoms was studied and clear distortion has been seen in both the real and imaginary parts of the electric susceptibility. With increasing the Rabi frequency of the laser pulse that in resonance with the lower transition the distortion will produce a new peak in the electric susceptibility parts, both the real and imaginary ones [14].

In this paper we have studied the effect of changing Rabi frequency on the electric susceptibility of the six-levels inverted-Y atomic configuration interacts with three laser fields shown in figure(1). The analytical model is applied to ^{87}Rb atom.

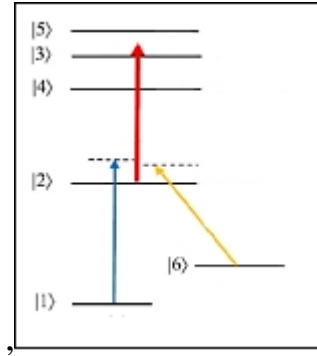


Figure (1) Six-levels Inverted-Y configuration

The transition $|1\rangle \leftrightarrow |2\rangle$ is driven by a weak probe laser field of frequency ω_p , and associated Rabi frequency Ω_p of the first pulse in the resonance of the lower transition, The transition $|6\rangle \leftrightarrow |2\rangle$ is interacted with a signal laser field of frequency ω_s , and Rabi frequency Ω_s . A strong coupling laser field with frequency ω_c and Rabi frequency Ω_c simultaneously couples transitions between the state $|2\rangle$, and three closely spaced states $|3\rangle$, $|4\rangle$ and $|5\rangle$. The frequency separations between the levels $|3\rangle$ - $|4\rangle$ and $|5\rangle$ - $|3\rangle$ are δ_1 and δ_2 , respectively

Theoretical Treatment

The non-linear response of a material system to an applied optical wave can be described by expressing the material polarization as a power series expansion in the electric field. The Hamiltonian H for the system can be written as [14]:

$$\hat{H} = \hat{H}_0 + \hat{H}_I \quad (1)$$

where H_0 describes the Hamiltonian for atom without presenting the electric field of the light, which is the laser. H_1 is the Hamiltonian of the interaction with the electric field of the laser. Now for six states $|n\rangle$ with the condition:

$$\sum_{n=1}^6 |n\rangle\langle n| = \hat{I} \quad , \quad \langle n|m\rangle = \delta_{nm} \quad (2)$$

The Hamiltonian H_0 can be written:

$$H_0 = \left(\sum_{n=1}^6 |n\rangle\langle n| \right) \hbar\omega_n \left(\sum_{n=1}^6 |n\rangle\langle n| \right)$$

$$H_0 = \begin{bmatrix} \hbar\omega_1 & 0 & 0 & 0 & 0 & 0 \\ 0 & \hbar\omega_2 & 0 & 0 & 0 & 0 \\ 0 & 0 & \hbar\omega_3 & 0 & 0 & 0 \\ 0 & 0 & 0 & \hbar\omega_4 & 0 & 0 \\ 0 & 0 & 0 & 0 & \hbar\omega_5 & 0 \\ 0 & 0 & 0 & 0 & 0 & \hbar\omega_6 \end{bmatrix} \quad (3)$$

The electric field equation of the three used lasers is:

$$E = \xi_{sp} \cos(\omega_p t) + \xi_c \cos(\omega_c t) + \xi_s \cos(\omega_s t) + c.c \quad (4)$$

Where ξ_p, ξ_c, ξ_s , are the amplitudes of the laser fields that has frequencies $\omega_p, \omega_c, \omega_s$

In the frame of rotating wave approximation, the interaction Hamiltonian H_1 can be written as:

$$H_1 = -\frac{1}{2} \times \begin{bmatrix} 0 & \xi_p \hat{P}_{12} e^{i\omega_p t} & 0 & 0 & 0 & 0 \\ \xi_p \hat{P}_{21} e^{-i\omega_p t} & 0 & \xi_c \hat{P}_{23} e^{i\omega_c t} & \xi_c \hat{P}_{24} e^{i\omega_c t} & \xi_c \hat{P}_{25} e^{i\omega_c t} & \xi_s \hat{P}_{26} e^{i\omega_s t} \\ 0 & \xi_c \hat{P}_{32} e^{-i\omega_c t} & 0 & 0 & 0 & 0 \\ 0 & \xi_c \hat{P}_{42} e^{-i\omega_c t} & 0 & 0 & 0 & 0 \\ 0 & \xi_c \hat{P}_{52} e^{-i\omega_c t} & 0 & 0 & 0 & 0 \\ 0 & \xi_s \hat{P}_{62} e^{-i\omega_s t} & 0 & 0 & 0 & 0 \end{bmatrix} \quad (5)$$

with the elements ρ_{nm} of the dipole operator $\rho = q\hat{r}$ that satisfy the condition $\rho_{nm} = \rho_{nm}^* = \langle n|\rho|m\rangle$, The Rabi frequencies defined as: $\Omega_p = \frac{\xi_p|\hat{p}_{12}|}{\hbar}$, $\Omega_c = \frac{\xi_c|\hat{p}_{25}|}{\hbar}$, $\Omega_s = \frac{\xi_s|\hat{p}_{62}|}{\hbar}$.

This gives the interaction Hamiltonian with Rabi frequencies terms as:

$$H_1 = -\frac{\hbar}{2} \times \begin{bmatrix} 0 & \Omega_p e^{i\varphi_p} e^{i\omega_p t} & 0 & 0 & 0 & 0 \\ \Omega_p e^{-i\varphi_p} e^{-i\omega_p t} & 0 & \Omega_c e^{i\varphi_c} e^{i\omega_c t} & \Omega_c e^{i\varphi_c} e^{i\omega_c t} & \Omega_c e^{i\varphi_c} e^{i\omega_c t} & \Omega_s e^{i\varphi_s} e^{i\omega_s t} \\ 0 & \Omega_c e^{-i\varphi_c} e^{-i\omega_c t} & 0 & 0 & 0 & 0 \\ 0 & \Omega_c e^{-i\varphi_c} e^{-i\omega_c t} & 0 & 0 & 0 & 0 \\ 0 & \Omega_c e^{-i\varphi_c} e^{-i\omega_c t} & 0 & 0 & 0 & 0 \\ 0 & \Omega_s e^{-i\varphi_s} e^{-i\omega_s t} & 0 & 0 & 0 & 0 \end{bmatrix} \quad (6)$$

Using eq. (3) and (6), we can rewrite eq.(1) as:

$$\hat{H} = \frac{\hbar}{2} \times \begin{bmatrix} 2\omega_1 & -\Omega_p e^{i\varphi_p} e^{i\omega_p t} & 0 & 0 & 0 & 0 \\ -\Omega_p e^{-i\varphi_p} e^{-i\omega_p t} & 2\omega_2 & -\Omega_c e^{i\varphi_c} e^{i\omega_c t} & -\Omega_c e^{i\varphi_c} e^{i\omega_c t} & -\Omega_c e^{i\varphi_c} e^{i\omega_c t} & -\Omega_s e^{i\varphi_s} e^{i\omega_s t} \\ 0 & -\Omega_c e^{-i\varphi_c} e^{-i\omega_c t} & 2\omega_3 & 0 & 0 & 0 \\ 0 & -\Omega_c e^{-i\varphi_c} e^{-i\omega_c t} & 0 & 2\omega_4 & 0 & 0 \\ 0 & -\Omega_c e^{-i\varphi_c} e^{-i\omega_c t} & 0 & 0 & 2\omega_5 & 0 \\ 0 & -\Omega_s e^{-i\varphi_s} e^{-i\omega_s t} & 0 & 0 & 0 & 2\omega_6 \end{bmatrix} \quad (7)$$

Using the co-rotating frame, the time independent Hamiltonian becomes:

$$\tilde{H} = \frac{\hbar}{2} \begin{bmatrix} 2(\omega_1 + \omega_p) & -\Omega_p & 0 & 0 & 0 & 0 \\ -\Omega_p & 2(\omega_2 + \omega_c) & -\Omega_c & -\Omega_c & -\Omega_c & -\Omega_s \\ 0 & -\Omega_c & 2\omega_3 & 0 & 0 & 0 \\ 0 & -\Omega_c & 0 & 2\omega_4 & 0 & 0 \\ 0 & -\Omega_c & 0 & 0 & 2\omega_5 & 0 \\ 0 & -\Omega_s & 0 & 0 & 0 & 2(\omega_6 + \omega_s) \end{bmatrix} \quad (8)$$

The Hamiltonian in terms of the detuning: $\Delta_p, \Delta_c, \Delta_s$ where: $\Delta_p = \omega_p - \omega_2 + \omega_1$, $\Delta_c = \omega_c - \omega_2 + \omega_5$, $\Delta_s = \omega_s - \omega_6 + \omega_2$ gives:

$$\tilde{H} = \frac{\hbar}{2} \begin{bmatrix} 0 & -\Omega_p & 0 & 0 & 0 & 0 \\ -\Omega_p & 2(\Delta_p - \Delta_s) & -\Omega_c & -\Omega_c & -\Omega_c & -\Omega_s \\ 0 & -\Omega_c & 2(\Delta_p - \Delta_c) & 0 & 0 & 0 \\ 0 & -\Omega_c & 0 & 2(\Delta_p - \Delta_c + \delta_1) & 0 & 0 \\ 0 & -\Omega_c & 0 & 0 & 2(\Delta_p - \Delta_c - \delta_2) & 0 \\ 0 & -\Omega_s & 0 & 0 & 0 & 0 \end{bmatrix} \quad (9)$$

On the other hand, the density matrix can be defined as:

$$\rho = \sum_n P_n |n\rangle\langle n| \quad (10)$$

where P_n is the probability of the occupation of the system in case n . The Von Neumann equation $\dot{\rho} = \frac{-i}{\hbar} [H, \rho]$, for system under the study, using eq. (9) and eq. (10), the Von Neumann equation is:

$$\dot{\rho}_{ij} = \sum_n \left[-\frac{i}{\hbar} (H_{ik}\rho_{kj} - \rho_{ik}H_{kj}) + \frac{1}{2} (\Gamma_{ik}\rho_{kj} + \rho_{ik}\Gamma_{kj}) \right]$$

$$\dot{\rho}_{21} = \dot{\rho}_{12}^* = [i\Delta_p - \gamma_{21}]\rho_{21} - \frac{i}{2}\Omega_p - \frac{i}{2}\Omega_c a_{32}\rho_{31} - \frac{i}{2}\Omega_c a_{42}\rho_{41} - \frac{i}{2}\Omega_c a_{52}\rho_{51} - \frac{i}{2}\Omega_s \rho_{61}$$

$$\dot{\rho}_{31} = \dot{\rho}_{13}^* = [i(\Delta_c + \Delta_p) - \gamma_{31}]\rho_{31} + \frac{i}{2}\Omega_p \rho_{32} - \frac{i}{2}\Omega_c a_{32}\rho_{21}$$

$$\dot{\rho}_{41} = \dot{\rho}_{14}^* = [i(\Delta_c + \Delta_p + \delta_1) - \gamma_{41}]\rho_{41} + \frac{i}{2}\Omega_p \rho_{42} - \frac{i}{2}\Omega_c a_{42}\rho_{21}$$

$$\dot{\rho}_{51} = \dot{\rho}_{15}^* = [i(\Delta_c + \Delta_p - \delta_2) - \gamma_{51}]\rho_{51} + \frac{i}{2}\Omega_p \rho_{52} - \frac{i}{2}\Omega_c a_{52}\rho_{21}$$

$$\dot{\rho}_{61} = \dot{\rho}_{16}^* = [i(\Delta_s - \Delta_p) - \gamma_{61}]\rho_{61} + \frac{i}{2}\Omega_p \rho_{62} - \frac{i}{2}\Omega_s \rho_{21}$$

$$\dot{\rho}_{32} = \dot{\rho}_{23}^* = [i\Delta_c - \gamma_{32}]\rho_{32} + \frac{i}{2}\Omega_p \rho_{31} + \frac{i}{2}\Omega_c a_{42}\rho_{34} + \frac{i}{2}\Omega_c a_{52}\rho_{35} + \frac{i}{2}\Omega_s \rho_{36}$$

$$\dot{\rho}_{42} = \dot{\rho}_{24}^* = [i(\Delta_c + \delta_1) - \gamma_{42}]\rho_{42} + \frac{i}{2}\Omega_p \rho_{41} + \frac{i}{2}\Omega_c a_{32}\rho_{43} + \frac{i}{2}\Omega_c a_{52}\rho_{45} + \frac{i}{2}\Omega_s \rho_{46}$$

$$\dot{\rho}_{52} = \dot{\rho}_{25}^* = [i(\Delta_c - \delta_2) - \gamma_{52}] \rho_{52} + \frac{i}{2} \Omega_p \rho_{51} + \frac{i}{2} \Omega_c a_{32} \rho_{53} + \frac{i}{2} \Omega_c a_{42} \rho_{54} + \frac{i}{2} \Omega_s \rho_{56}$$

$$\dot{\rho}_{62} = \dot{\rho}_{26}^* = [i\Delta_s - \gamma_{62}] \rho_{62} + \frac{i}{2} \Omega_p \rho_{61} + \frac{i}{2} \Omega_c a_{32} \rho_{63} + \frac{i}{2} \Omega_c a_{42} \rho_{64} + \frac{i}{2} \Omega_c a_{52} \rho_{65}$$

$$\dot{\rho}_{43} = \dot{\rho}_{34}^* = [-i\delta_1 - \gamma_{43}] \rho_{43} + \frac{i}{2} \Omega_c a_{32} \rho_{42} - \frac{i}{2} \Omega_c a_{42} \rho_{23}$$

$$\dot{\rho}_{53} = \dot{\rho}_{35}^* = [-i\delta_2 - \gamma_{53}] \rho_{53} + \frac{i}{2} \Omega_c a_{32} \rho_{52} - \frac{i}{2} \Omega_c a_{52} \rho_{23}$$

$$\dot{\rho}_{63} = \dot{\rho}_{36}^* = [i(\Delta_s - \Delta_c) - \gamma_{36}] \rho_{63} + \frac{i}{2} \Omega_c a_{32} \rho_{62} - \frac{i}{2} \Omega_s \rho_{23}$$

$$\dot{\rho}_{54} = \dot{\rho}_{45}^* = [-i(\delta_1 + \delta_2) - \gamma_{54}] \rho_{54} + \frac{i}{2} \Omega_c a_{42} \rho_{52} - \frac{i}{2} \Omega_c a_{52} \rho_{24}$$

$$\dot{\rho}_{64} = \dot{\rho}_{46}^* = [i(\Delta_c - \Delta_s + \delta_1) - \gamma_{46}] \rho_{64} + \frac{i}{2} \Omega_c a_{42} \rho_{62} - \frac{i}{2} \Omega_s \rho_{24}$$

$$\dot{\rho}_{65} = \dot{\rho}_{56}^* = [i(\Delta_c - \Delta_s - \delta_1) - \gamma_{56}] \rho_{65} + \frac{i}{2} \Omega_c a_{52} \rho_{62} - \frac{i}{2} \Omega_s \rho_{25} \quad (11)$$

For N atoms, the polarization using the density matrix is:
 $P(r) = N \langle \hat{p}(r) \rangle = N Tr(\rho \hat{p})$

$$P = N Tr \times$$

$$\left(\begin{array}{cccccc} \rho_{11} & \rho_{12} & \rho_{13} & \rho_{14} & \rho_{15} & \rho_{16} \\ \rho_{21} & \rho_{22} & \rho_{23} & \rho_{24} & \rho_{25} & \rho_{26} \\ \rho_{31} & \rho_{32} & \rho_{33} & \rho_{34} & \rho_{35} & \rho_{36} \\ \rho_{41} & \rho_{42} & \rho_{43} & \rho_{44} & \rho_{45} & \rho_{46} \\ \rho_{51} & \rho_{52} & \rho_{53} & \rho_{54} & \rho_{55} & \rho_{56} \\ \rho_{61} & \rho_{62} & \rho_{63} & \rho_{64} & \rho_{65} & \rho_{66} \end{array} \right) \left(\begin{array}{cccccc} 0 & \hat{P}_{12} & 0 & 0 & 0 & 0 \\ \hat{P}_{21} & 0 & \hat{P}_{23} & \hat{P}_{24} & \hat{P}_{25} & \hat{P}_{26} \\ 0 & \hat{P}_{32} & 0 & 0 & 0 & 0 \\ 0 & \hat{P}_{42} & 0 & 0 & 0 & 0 \\ 0 & \hat{P}_{52} & 0 & 0 & 0 & 0 \\ 0 & \hat{P}_{62} & 0 & 0 & 0 & 0 \end{array} \right) \quad (12)$$

and polarization will be simply rewritten as:

$$P = N(\rho_{12} \hat{P}_{21} + \rho_{21} \hat{P}_{12} + \rho_{23} \hat{P}_{32} + \rho_{24} \hat{P}_{42} + \rho_{25} \hat{P}_{52} + \rho_{26} \hat{P}_{62} + \rho_{32} \hat{P}_{23} + \rho_{42} \hat{P}_{24} + \rho_{52} \hat{P}_{25} + \rho_{62} \hat{P}_{26}) \quad (13)$$

From the polarization P we can calculate the electric susceptibility for the system:

$$\chi = \frac{2N|\tilde{P}_{21}|}{\epsilon_0 \xi_p} \left(\frac{-\Omega_p \Delta_p + i\gamma_{12} \Omega_p}{2(A + iB)} \right) \quad (14)$$

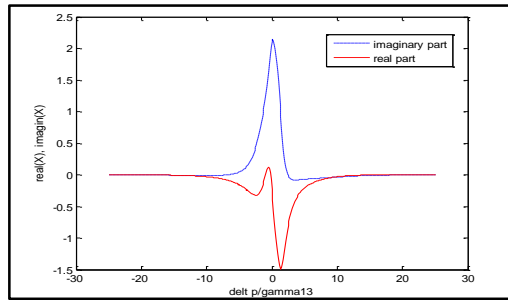
From eq.(14) the real and imaginary parts are:

$$\chi_{real} = \frac{2N|\tilde{P}_{21}|}{\epsilon_0 \xi_p} \left(\frac{\Omega_p \Delta_p A + \gamma_{12} \Omega_p B}{A^2 + B^2} \right) \quad (15)$$

$$\chi_{imaginary} = i \frac{2N|\tilde{P}_{21}|}{\epsilon_0 \xi_p} \left(\frac{\gamma_{12} \Omega_p A - \Omega_p \Delta_p B}{A^2 + B^2} \right) \quad (16)$$

Results and Discussion

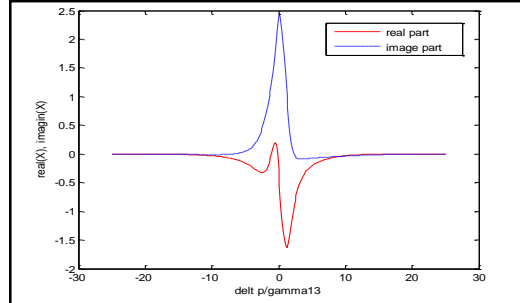
In this section, we apply the calculation results to ^{87}Rb atom with the states shown in figure (1). and with the help of matlab software, we have calculated the electric susceptibility for different values of Ω_c and Ω_s . Figure (2) represents the real and imaginary parts of the electric susceptibility with $\Omega_c = 1 \text{ MHz}$, $\Omega_p = 1.5 \text{ MHz}$, $\Omega_s = 0.9 \text{ MHz}$.



Figure(2): The real and imaginary parts of the electric susceptibility ($\Omega_c = 1 \text{ MHz}$)

$$\Delta_p/\gamma_{13}, \Omega_p = 1.5 \text{ MHz}, \Omega_s = 0.9 \text{ MHz}, \Delta_c = 0.6 \text{ MHz}, \Delta_s = 0.8 \text{ MHz}$$

With increasing the value of Rabi frequency Ω_c between levels $|2\rangle$ – $|5\rangle$ at the same value of Ω_p and Ω_s , we notice increase in the values of both real and imaginary parts and the behavior stay the same. . Figure (3) shows that at $\Omega_c = 2 \text{ MHz}$ with the same parameters.



Figure(3): The real and imaginary parts of the electric susceptibility ($\Omega_c = 2\text{MHz}$)

$$\Omega_s = 0.9 \text{ MHz}, \Delta_c = 0.6 \text{ MHz}, \Delta_s = 0.8 \text{ MHz}, \Delta_p/\gamma_{13}, \Omega_p = 1.5 \text{ MHz}$$

In figure (4) the increase in the value of both parts of the electric susceptibility becomes much clearer as we increase Ω_c to 4MHz .

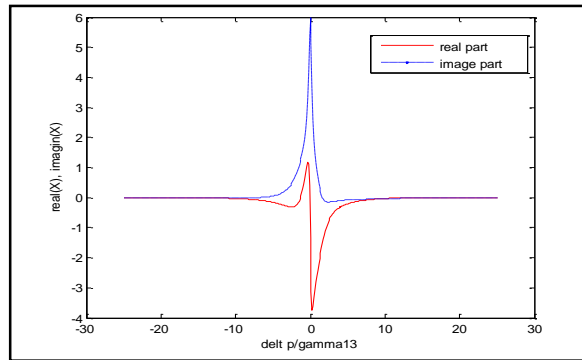


Figure (4) The real and imaginary parts of the electric susceptibility ($\Omega_c = 4\text{MHz}$)

$$\Omega_s = 0.9 \text{ MHz}, \Delta_c = 0.6 \text{ MHz}, \Delta_s = 0.8 \text{ MHz}, \Delta_p/\gamma_{13}, \Omega_p = 1.5 \text{ MHz}$$

For different values of Rabi frequency, the real and imaginary parts of the electric susceptibility drawn in figure (5) figure (6) to prove the conclusion that we have reach.

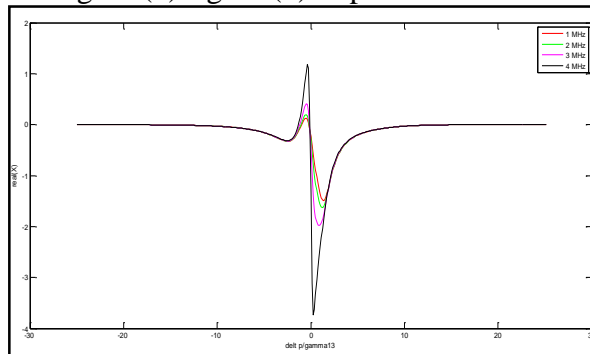


Figure (5) The real part of the electric susceptibility

$$\Delta_c = 0.6 \text{ MHz}, \Delta_s = 0.9 \text{ MHz}, \Delta_p/\gamma_{13}, \Omega_p = 1.5 \text{ MHz} (\Omega_c = 1, 2, 3, 4 \text{ MHz})$$

$$\gamma_{16} = 0.8 \text{ MHz}, \gamma_{12} = 1 \text{ MHz}, \gamma_{13} = 0.8 \text{ MHz}, \gamma_{14} = 2 \text{ MHz}, \gamma_{15} = 0.6 \text{ MHz}$$

$$1.5 \text{ MHz}, \xi_p = 5 \text{ V/m}$$

Also we have calculated the electric susceptibility for different values of Ω_s . figure(7) represents the real and imaginary parts of the electric susceptibility with $\Omega_s = 1 \text{ MHz}$, $\Omega_p = 1.5 \text{ MHz}$, $\Omega_c = 0.9 \text{ MHz}$ rabi frequency Ω_s at the same value of Ω_p and Ω_c . Figure(8) shows that at $\Omega_s = 2 \text{ MHz}$ with the same parameters, we notice decrease in the values of both real and imaginary parts and a distortion starts to appear on both real and imaginary parts. In figure (9) the decrease in the value of both parts of the electric susceptibility becomes much clearer as we increase Ω_s to 4 MHz .

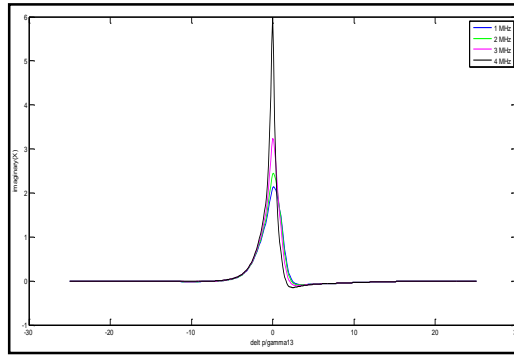


Figure (6) The imaginary part of the electric susceptibility ($\Omega_c = 1, 2, 3, 4 \text{ MHz}$)

$$\Delta_c = 0.6 \text{ MHz}, \Delta_s = 0.8 \text{ MHz}, \gamma_{12} = 1 \text{ MHz}, \Omega_s = 0.9 \text{ MHz}, \Delta_p/\gamma_{13}, \Omega_p = 1.5 \text{ MHz}$$

$$\gamma_{16} = 1.5 \text{ MHz}, \xi_p = 5 \text{ V/m}, \gamma_{13} = 0.8 \text{ MHz}, \gamma_{14} = 2 \text{ MHz}, \gamma_{15} = 0.6 \text{ MHz}$$

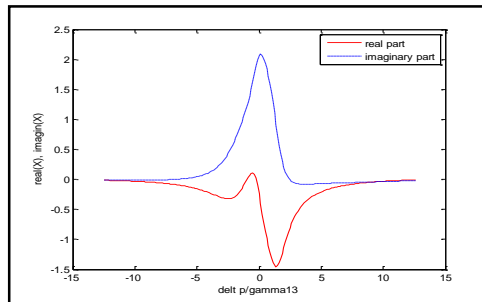
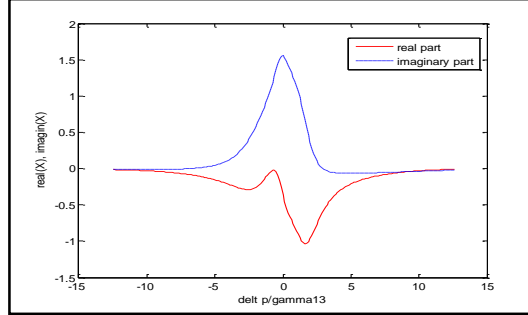


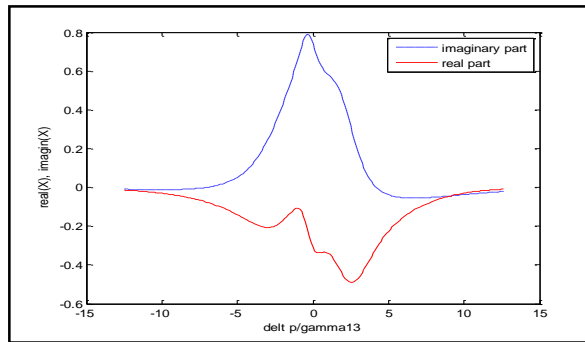
Figure (7): The real and imaginary parts of the electric susceptibility ($\Omega_s = 1 \text{ MHz}$)

$$\Delta_c = 0.6 \text{ MHz}, \Delta_s = 0.8 \text{ MHz}, \Omega_c = 0.9 \text{ MHz}, \Delta_p/\gamma_{13}, \Omega_p = 1.5 \text{ MHz}$$



Figure(8): The real and imaginary parts of the electric susceptibility ($\Omega_s = 2\text{MHz}$)
 $\Delta_p/\gamma_{13}, \Omega_p = 1.5\text{MHz}$

$$\Delta_c = 0.6 \text{ MHz}, \Delta_s = 0.8 \text{ MHz}, \Omega_c = 0.9 \text{ MHz},$$



Figure(9): The real and imaginary parts of the electric susceptibility ($\Omega_s = 4\text{MHz}$)
 $\Delta_c = 0.6\text{MHz}, \Delta_s = 0.8\text{MHz}, \Omega_c = 0.9\text{MHz}, \Delta_p/\gamma_{13}, \Omega_p = 1.5\text{MHz}$

For different values of Rabi frequency Ω_s , the real and imaginary parts of the electric susceptibility drawn in figure (10) to prove the conclusion that we have reach.

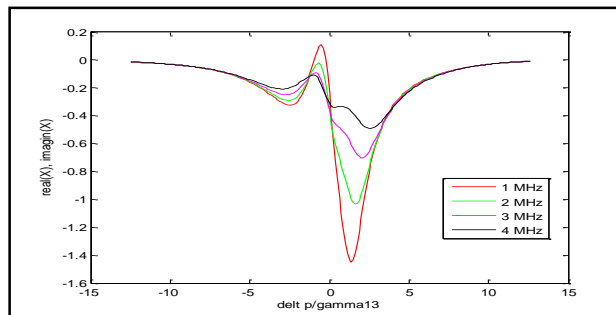


Figure (10) The real part of the electric susceptibility ($\Omega_s = 1, 2, 3, 4\text{MHz}$)
 $\Delta_c = 0.6 \text{ MHz}, \Delta_s = 0.8 \text{ MHz}, \gamma_{13} = 0.8 \text{ MHz}, \gamma_{14} = 2 \text{ MHz}, \Omega_c = 0.9 \text{ MHz}, \Omega_p = 1.5 \text{ MHz}$
 $\gamma_{12} = 1\text{MHz}, \gamma_{16} = 1.5\text{MHz}, \xi_p = 5 \text{ V/m}, \gamma_{15} = 0.6\text{MHz}$

Conclusion

Optical Bloch equations were used as the main tool to get the final shape of the model to treat the model. In this work we present a theoretical study of the non-linear optical properties of materials as a result of their interaction with laser radiation in resonance state. Density matrix was used in our formulation of Optical Bloch Equation. These equations were solved using Matlab program for Six-levels Inverted-Y Atomic Systems. A formula for calculation of electrical susceptibility was obtained. with increasing Ω_c the real and imaginary parts of the electric susceptibility have also increased gradually which effects the index of refraction of the medium (real part), and the absorption window (described by the imaginary part). Moreover when increasing Ω_s the real and imaginary parts of the electric susceptibility decreased and we noticed that with increasing the value of the signal laser field related to transition $|2\rangle \leftrightarrow |6\rangle$ a distortion starts to appear on both real and imaginary parts.

References:

- [1] Lechner, D., Pennetta, R., Blaha, M., Schneeweiss, P., Rauschenbeutel, A., & Volz, J. (2023). Light-matter interaction at the transition between cavity and waveguide QED. *Physical Review Letters*, 131(10), 103603.
- [2] M. Fleischhauer and M. D. Lukin, \Dark-State Polaritons in Electromagnetically Induced Transparency,"*Phys. Rev. Lett.*, **84**, 5094-5097 (2000).
- [3] M. Fleischhauer, A. Imamoglu, and J. P. Marangos, \Electromagnetically induced transparency: Optics in coherent media,"*Revs. Mod. Phys.* **77**, 633- 673(2005).
- [4] M. O. Scully and M. S. Zubairy,(Quantum optics) *Cambridge University Press*,2006
- [5] Chun-Fei, L., Xiao-Xu, D., & Yu-Xiao, W. (2000). Nonlinear absorption and refraction in multilevel organic molecular system. *Chinese Physics Letters*, 17(8), 574.
- [6] Semin, S., Li, X., Duan, Y., & Rasing, T. (2021). Nonlinear optical properties and applications of fluorenone molecular materials. *Advanced Optical Materials*, 9(23), 2100327.
- [7] Erickson, W. W. (2012). Electromagnetically Induced Transparency (Doctoral dissertation, Reed College).
- [8] Hau, L. V., Harris, S. E., Dutton, Z., & Behroozi, C. H. (1999). Light speed reduction to 17 metres per second in an ultracold atomic gas. *Nature*, 397(6720), 594-598.

- [9].Kai, W., Ying, G., and Qi-Huang, G. (2007). Stimulated emission and multi-peaked absorption in a four level N-type atom. Chinese Physics, 16(1), 130.
- [10]Safari, L., Iablonskyi, D., and Fratini, F. (2014). Double electromagnetically induced transparency in a Y-type atomic system. The European Physical Journal D, 68(2), 1-8
- [11]Bharti, V., and Natarajan, V. (2015). Study of a four-level system in vee+ ladder configuration. Optics Communications, 356, 510-514. physics. atom-ph
- [12]Gu, Y., Wang, L., Wang, K., Yang, C., and Gong, Q. (2005). Coherent population trapping and electromagnetically induced transparency in a five-level M-type atom. Journal of Physics B: Atomic, Molecular and Optical Physics, 39(3), 463.
- [13]An, N. L. T., Khoa, D. X., Sau, V. N., and Bang, N. H. (2019). Manipulating giant cross-Kerr nonlinearity at multiple frequencies in an atomic gaseous medium. JOSA B, 36(10), 2856-2862.
- [14]Abuzariba, S., Mafaa, E. (2017). The effect of the rabi frequency on the Electric susceptibility for Λ -type three level atom when it interacts with laser beam.